

1 **Title:**

2 **Quantification of Adeno-Associated Virus with Safe Nucleic Acid Dyes**

3

4 **Running title:**

5 Using Safe Nucleic Acid Dyes to Titer Adeno-Associated Virus

6

7 Jian Xu<sup>1</sup>, Steven H DeVries<sup>1</sup> and Yongling Zhu<sup>1</sup>

8

9 <sup>1</sup>Department of Ophthalmology

10 Northwestern University Feinberg School of Medicine,

11 Chicago, IL 60611, USA

12

13 e-mail: Jian Xu jian-xu@northwestern.edu

14 Steven H DeVries steven.devries@northwestern.edu

15 Yongling Zhu yongling-zhu@northwestern.edu

16

17

18 Correspondence to: Yongling Zhu, PhD

19 Department of Ophthalmology

20 Northwestern University Feinberg School of Medicine

21 303 E Chicago Ave, Tarry 5-723

22 Chicago IL 60611, USA

23 Tel: 312-503-2141

24

## 25 **Abstract**

26 Adeno-associated virus (AAV) is the most commonly used viral vector for both  
27 biological and gene therapeutic applications<sup>1</sup>. Although many methods have been  
28 developed to measure quantity attributes of AAV, they are often technically challenging  
29 and time consuming. Here we report a method to titer AAV with GelGreen® dye, a safe  
30 green fluorescence nucleic acid dye recently engineered by Biotium company (Fremont,  
31 CA). This method, hereinafter referred to as GelGreen method, provides a fast (~ 30  
32 minutes) and reliable strategy for AAV titration. To validate GelGreen method, we  
33 measured genome titer of an AAV reference material AAV8RSM and compared our  
34 titration results with those determined by Reference Material Working Group (ARMWG).  
35 We showed that GelGreen results and capsid Elisa results are comparable to each  
36 other. We also showed that GelRed® dye, a red fluorescence dye from Biotium, can be  
37 used to directly “visualize” AAV genome titer on a conventional gel imager, presenting  
38 an especially direct approach to estimate viral quantity. In summary, we described a  
39 technique to titer AAV by using new generation of safe DNA dyes. This technique is  
40 simple, safe, reliable and cost-efficient. It has potential to be broadly applied for  
41 quantifying and normalizing AAV viral vectors.

42

## 43 **Introduction**

44 AAV is a small single-stranded DNA virus belonging to parvovirus family<sup>2</sup>.  
45 Features such as low toxicity, high safety, long-term expression and efficient  
46 transduction of both dividing and non-dividing cells have made AAV the most frequently  
47 used viral vector in biological studies<sup>3-5</sup>. Over the last two decades, AAV vector has also  
48 emerged as the most common vehicle for gene therapy<sup>1, 6</sup>. Back in 1995, an AAV

49 vehicle was first used to treat cystic fibrosis in a human patient<sup>7</sup>. In 2008, three clinical  
50 trials using AAV vectors to treat Leber's congenital amaurosis were published<sup>8-10</sup>. As of  
51 to date, more than two hundreds clinical trials involving AAV have been conducted,  
52 whereby AAV vectors have shown great promise in treating different human diseases.

53 Recombinant AAV (rAAV) can now be packaged and purified quite routinely in  
54 laboratories, but their titers can vary largely, depending on packaging and purification  
55 methods and scales of production. Therefore it is imperative to establish accurate titers  
56 of rAAVs to ensure appropriate dosing. Many analytical methods, designed to measure  
57 either the physical or infectious titer of rAAV, have been developed. Among these are,  
58 for example, the dot blot hybridization<sup>11</sup>, enzyme-linked immunosorbent assay (Elisa)<sup>12</sup>,  
59 <sup>13</sup>, Electron microscopy (EM)<sup>14</sup>, qPCR<sup>15-17</sup>, optical density<sup>18</sup>, DNA dye binding assay<sup>19</sup>  
60 SDS-PAGE gel assay<sup>20, 21</sup>, TCID<sub>50</sub> (50% Tissue Culture Infective Dose)<sup>22</sup>, replication  
61 center assay (RCA)<sup>23</sup> and infectious center assay (ICA) assays<sup>24</sup>. Apparently each  
62 method has its own advantages and limitations. In the last several years, qPCR method  
63 has emerged as one of the most popular choices among labs, mostly due to its high  
64 sensitivity and broad dynamic range. But the qPCR method, like many others, also  
65 presents drawbacks. For instance, qPCR method is rather labor intensive. It is highly  
66 sensitive to experimental conditions, making it susceptible to errors. Factors such as  
67 PCR primers, reagents, equipment and DNA standards etc., can all significantly  
68 influence the test results<sup>25, 26</sup>. Because of that, significant inter- and intra- laboratory  
69 variations were often reported<sup>27</sup>. To overcome some of these issues, AAV titration  
70 method based on droplet digital PCR (ddPCR) was developed<sup>27</sup>. ddPCR is an endpoint  
71 PCR approach with the capability of measuring absolute number of DNA targets. Unlike  
72 qPCR, ddPCR is independent of reference materials and is less sensitive to inhibitors of

73 PCR reactions, making it more accurate for measuring AAV titers<sup>28</sup>. However, ddPCR  
74 titration method is not widely used. Perhaps the requirement for special instrument and  
75 relatively high labor intensity have limited its broad application.

76 rAAVs can also be tittered by measuring their DNA contents more directly. For  
77 example, Cell Biolabs (San Diego, CA) has designed a commercial AAV titration kit  
78 (QuickTiter™ AAV Quantitation kit) based on quantifiable binding of DNA dye (CyQuant  
79 GR) to rAAV genome. Similarly, picoGreen, another sensitive DNA dye, has also been  
80 used to measure AAV titer based on the same principle<sup>19</sup>. A major advantage of DNA  
81 dye based assays is that they can be completed within 2-3 hours, much shorter than  
82 many other methods. Also, DNA dye-based assays was reported to have much less  
83 intra- and inter-assay variability as compared to dot blot and qPCR methods<sup>19</sup>. Notably,  
84 both CyQuant GR dye and picoGreen are membrane permeable dyes belonging to  
85 cyanine dye family. While CyQuant GR is often used in cell proliferation assays<sup>29</sup>,  
86 picoGreen dye is often used for quantifying double stranded (ds) DNA<sup>30, 31</sup>.

87 In recent years, several safe nucleic acid dyes have been developed, such as  
88 Gelgreen® and Gelred® from Biotium (Fremont, CA, USA), SYBRsafe and SYBRgold  
89 from Thermo-Fisher Scientific (Waltham, MA, USA) and Diamond™ from Promega  
90 (Madison, WI, USA). These dyes are now widely available as more and more labs are  
91 choosing them to replace ethidium bromide to stain DNA and RNA in gels. Compared  
92 with CyQuant GR dye and picoGreen dyes, these new dyes are more affordable.  
93 Importantly, they are membrane impermeant, making them safer to use and more  
94 friendly to environment.

95 In an effort to develop a safe, simple and reliable method for measuring AAV  
96 concentrations, we wondered if we could take advantage of the newly developed safe

97 nucleic acid dyes, such as GelRed® and GelGreen®. According to Biotium, both  
98 GelRed® and GelGreen® can readily detect 1 ng of DNA in gel, with some users being  
99 able to detect bands containing less than 0.1 ng DNA. If these claims are true, then  
100 GelRed® and GelGreen® should at least be capable of detecting 3 - 4  $\mu$ l of AAV at titer  
101 of  $1 \times 10^{11}$  GC/ml, which contains  $\sim 1$  ng DNA (GC stands for genome copy; equations  
102 are provided in the method section). This level of sensitivity should be sufficient for most  
103 AAV samples as standard laboratory protocols typically produce rAAVs with titers one to  
104 two logs higher than  $1 \times 10^{11}$  GC/ml.

105         Here we report a method to measure AAV titer with GelGreen® and GelRed®.  
106 This method is fast, safe, reliable and cost-efficient. It produced similar result as  
107 compared to capsid Elisa method<sup>32</sup>. We believe this method could to be broadly useful  
108 in quantifying and normalizing AAV vectors.

109

## 110 **Materials and Methods**

### 111 **rAAV production and purification**

112 rAAVs were produced in-house using triple transfection methods<sup>33-36</sup>. The  
113 plasmids used for transfections were as follows: 1) cis-plasmid containing a gene  
114 expression cassette flanked by AAV2 inverted terminal repeats (ITRs); 2) trans-  
115 plasmids containing the AAV2 rep gene and AAV2 capsid protein genes; 3) adenovirus  
116 helper plasmid pAd $\Delta$ F6. rAAVs were purified by iodixanol gradient ultracentrifugation as  
117 previously described<sup>16, 37</sup>. rAAV serotype 8 Reference Standard Material (AAV8RSM)<sup>38</sup>  
118 was purchased from American Type Culture Collection (ATCC # VR-1816).

### 119 **Cytation 3 Plate reader**

120 Cytation 3 Multi-Mode plate reader from BioTek (Winooski, VT) was used for  
121 DNA binding assay. It was equipped with a 488 nm laser for excitation and a 528/20  
122 filter for emission. Gelgreen® was chosen to stain DNA because its excitation and  
123 emission spectrums are similar to GFP and it can be readily detected by virtually any  
124 plate readers.

### 125 **Gel imager**

126 We used a DNA gels imager (Gel Logic 200 Imaging System) from Kodac  
127 (Rochester, NY), combined with a UV light box, to visualize viral DNA stained with  
128 Gelred®. Digital images were acquired and analyzed by image J software as  
129 described<sup>39</sup> to provide a semi-quantitative analysis.

### 130 **Data Analysis**

131 Statistical analyses were conducted with Graphpad Prism software (San Diego,  
132 CA). Student's t-test and One-way ANOVA with Tukey's post hoc test was used for data

133 comparisons. Differences were considered significant when  $p < 0.05$ . Data are shown as  
134 mean  $\pm$  SD.

135 The limit of detection (LOD) is defined as the mean value of sample blanks plus 3  
136 standard deviations (SD). The limit of quantification (LOQ) is defined as mean value of  
137 sample blanks plus 10 SD.

138 A plasmid DNA, initially constructed as a cis-plasmid for making rAAV was used  
139 in this study as DNA standard. Its concentration was measured by NanoDrop™  
140 Spectrophotometers (ThermoFisher, Waltham, MA, USA). The amounts of DNA (ng) in  
141 viral samples, either lysed or unlysed, were determined by standard curves. We then  
142 calculated the amount of encapsided DNA as the difference between the values of lysed  
143 samples and un-lysed samples.

144 The following are equations for converting encapsided DNA (ng) to AAV titer  
145 (GC/ml):

$$(1) \quad AAV \text{ titer}(GC/ml) = \frac{(DNA \text{ mass in ng}) * (1.0E - 9)g * 6.022E23 \text{ mol}^{-1}}{MW * (volume \text{ in ul}) * (1E - 3)ml}$$

146 where,

$$(2) \quad MW = genome \text{ size (nt)} * 330 \text{ g/mol}$$

147

148 Note 1: 330 g/mol is the average mass of a single nucleotide (nt). Genome size  
149 of rAAV (ssDNA) is typically between 4000 to 5000 nt.

150 Note 2: If DNA sequence is available, MW of an AAV genome can be more  
151 precisely determined. For example, AAV8RSM was produced by pTR-UF-11 plasmid<sup>40</sup>.  
152 Based on its sequence, we calculated the MW of AAV8RSM's genome to be 1 334 245  
153 (g/mol). This number was used to compute titers of AAV8RSM in this report.

154

## 155 **Results**

### 156 **Detection of DNA by Gelgreen®**

157 To determine the detection limit and optimal concentration of Gelgreen dye, we  
158 carried out quantitative DNA binding assays using Cytation 3 plate reader. To set up the  
159 binding assay, we prepared several sets of DNA standards using a plasmid DNA. Each  
160 set of standard contains 12-point serial dilutions of DNA ranging from 0-50 ng. DNA  
161 standards were then transferred to 96-well plate containing GelGreen® diluted in  
162 phosphate-buffered saline (PBS) before fluorescence measurement.

163 Calibration plot of fluorescence intensity versus DNA is shown in Figure 1A  
164 (linear scale) and Figure 1B (logarithmic scale). Between 1/3000 to 1/100 000 dilution,  
165 GelGreen® readily responded to a wide range of DNA, showing linearity for DNA in the  
166 range of 0-50 ng, with all assays exhibiting acceptable correlation efficient ( $R^2$ ) of >99%  
167 (Figure 1A, 1B). However, at high concentrations of GelGreen® (1:500 and 1:1000),  
168 fluorescence signals no longer responded to DNA (Figure 1A, 1B). To view the effects  
169 of dye more directly, we re-plotted the data as fluorescence intensity vs. dye  
170 concentration in Figure 1C. This plot revealed a series of inverse bell-shaped dose-  
171 response curves for any given amount of DNA (0.78 - 50 ng), with their peak values all  
172 occurring at ~1/10 000 dye dilution and with sharp downslopes occurring after 1/3000.  
173 Thus in our assay, the optimal dye concentration for detecting DNA was 1/10 000,  
174 agreeing with manufacture's recommendation.

175 To assess the sensitivity of the DNA binding assay, we measured both the limit  
176 of detection (LOD) and the limit of quantification (LOQ) of GelGreen® at 1/10 000  
177 dilution. (Figure 1D). With the standard deviation (SD) to be 10.60 and mean value to be  
178 583 for sample blanks (n=3), we calculated the LOD and LOQ to be 611 and 690



179 respectively. Based on these values, we derived LOD to be 0.19 ng and LOQ to be and  
180 0.35 ng from standard curve (marked with dashes lines in Figure 1D). In addition, using  
181 t-test we found that 0.39 ng DNA was the lowest amount to achieve statistical  
182 significance when compared to sample blanks ( $707.70 \pm 26.03$  vs  $583 \pm 10.60$ ,  $n=3$ ,  
183  $p<0.01$ ). Thus, Gelgreen® - based DNA binding assay is sensitive enough to measure  
184 as low as 0.2 - 0.4 ng DNA.

185

### 186 **Release of viral DNA by heating**

187 AAV genome is encapsided. To measure it, one must first break apart viral  
188 capsids. Common methods for this purpose are proteinase K digestion<sup>27</sup> and heat  
189 inactivation<sup>18</sup>. Often Proteinase K digestion is proceeded by DNase I treatment to  
190 remove DNA contaminations<sup>25, 27</sup>. Heat inactivation is often performed around 70 °C in  
191 the presence of 0.05-0.1% SDS<sup>18</sup>. It usually takes one hour to perform these  
192 inactivation protocols.

193 In an effort to further shorten experimental time, we devised and tested two  
194 strategies for releasing viral DNA contents. The first strategy involves heating samples  
195 at high temperature of 95 °C, which can be done easily with standard PCR thermo-  
196 cycler. Meanwhile we also tested whether it is necessary to include SDS during heating  
197 process. In this experiment, we used an in-house produced rAAV sample packaged in  
198 capsid from serotype 2. We first diluted rAAV into 10 µl of PBS in PCR tubes then  
199 heated samples at 95 °C in thermo-cycler for various length of time. After heating and  
200 natural cooling, samples were transferred to 96-well plate containing 90 µl PBS and  
201 GelGreen® at 1/10 000 dilution for fluorescence measurement.

202           Results are shown in Figure 2A. We first inspected intrinsic dye signals (blanks)  
203 and compared that with signals of non-heated samples (see the blue line, 0 SDS).  
204 Sample blanks yielded signals of  $515.7 \pm 26.58$  (n=3), whereas the non-heated sample  
205 exhibited slightly higher fluorescence ( $647.3 \pm 16.80$ , n=3). The small difference here  
206 was thought to be caused by contamination of non-encapsided DNA in the AAV prep,  
207 which is quite common. Heating samples at 95°C caused a much larger increase of  
208 fluorescence signals, suggesting that contents of rAAV genome were released.  
209 Surprisingly, merely 5 minute of heating appeared to be sufficient, as longer heating (up  
210 to 20 minutes) produced no further increase of fluorescence. This observation implied  
211 that most of capsids, if not all, were already destroyed by heating after 5 minutes.

212           When samples (10 ul) were heated in the presence of 0.1% SDS, which yielded  
213 0.01% SDS in final volume of 100 ul (red line), fluorescence signals again peaked at 5  
214 minute. However these signals were significantly lower when compared to those without  
215 SDS (blue line). In an extreme case, when SDS was at final concentration of 0.1%  
216 (green line), the increase of fluorescence by heating was completely prevented (Figure  
217 2A).

218           To investigate the effect of SDS more carefully, we prepared four sets of DNA  
219 standard containing different amount of SDS and performed DNA binding assays.  
220 Results are summarized in Figure 2B. While small amount of SDS (0.001%) had little  
221 effect as compared to control, 0.01% SDS already caused significantly inhibition. At  
222 0.1% SDS, fluorescence responses completely vanished. Thus SDS must be kept low,  
223 otherwise will obstruct DNA binding assay. We advise that care should be taken when  
224 using GelGreen® to stain DNA in gels. Many GelGreen® users may not be aware that

225 high amount of SDS (0.5% - 1%) is often included in 10X DNA loading dyes, which  
226 could have significant negative impact on detecting DNA bands by GelGreen®.

227 In conclusion, we found that 5 minutes of heating at 95 °C in PBS provided a  
228 simple and efficient way to release viral DNA. Meanwhile we also found that not only  
229 was SDS unnecessary but it was also detrimental for DNA detection by GelGreen®.

230

### 231 **Release of viral DNA by alkaline lysis**

232 The second strategy we explored was the alkaline lysis. It is a very common  
233 molecular technique for protein and DNA denaturation, but it has rarely been used for  
234 lysing AAV particles<sup>17</sup>. We decided to test whether encapsulated viral DNA can be  
235 efficiently released by NaOH. Different amount of NaOH was tested for its lysing ability.  
236 The procedure is simple. We first treated viral samples (10 µl) with 2 µl of NaOH, we  
237 then added 2 µl of Tris buffer (PH 5.0) of two times the concentration of NaOH, to  
238 neutralize NaOH. Right after that we conducted DNA binding assay as described.

239 A dose-response curve of NaOH on fluorescence signals is shown in Figure 3A.  
240 Clearly, fluorescence signals were enhanced by NaOH, with large increases observed  
241 from samples treated with 15 mM to 125mM NaOH. It is likely that under these  
242 conditions viral particles were fully lysed. In comparison, 7.5 mM NaOH only caused a  
243 small fluorescence increase, suggesting that it only triggered a partial release. Based on  
244 the dose-response curve, we estimated the EC<sub>50</sub> of NaOH treatment to be ~12 mM.  
245 Also noticeable was a small decline of fluorescence when NaOH was above 125 mM.  
246 We suspected that high dose of NaOH/Tris treatment may either cause DNA damage or  
247 weaken DNA/dye interactions. In light of this observation, we consider proper range of  
248 NaOH to be between 30 mM to 125 mM.

249 Together we explored two methods to release viral DNA from capsids. Both  
250 methods can be done quickly and both appear to be fully effective. To be more  
251 assertive about their efficacies, we tested if combining two treatments could yield higher  
252 lysis than single treatment alone. Briefly, we either added NaOH (100 mM) to samples  
253 that have already been heated at 95 °C, or we subjected NaOH-treated samples to 95  
254 °C heating. As shown in Figure 3B, neither did NaOH (Purple) increase fluorescence to  
255 samples that have already been heated (Green), nor did heating (Black) enhance  
256 fluorescence of NaOH-treated samples (Orange). Together these results suggest that  
257 AAV were fully lysed by either of the two lysing methods alone, rendering the follow-up  
258 treatment nominal. In summary, heating method and alkaline method are both efficient  
259 and quick. Alkaline lysis is even easier to set up, giving itself a slight edge.

260

#### 261 **Titration of AAV8RSM by GelGreen method**

262 To validate GelGreen method for AAV titration, we measured titer of an AAV  
263 reference material (ARM) and compared our results to published results. The reference  
264 material was developed and characterized by ARMWG, for the purpose of normalizing  
265 titers of AAV vectors<sup>38, 41</sup>. Two ARMs, AAV2RSM and AAV8RSM, are available from  
266 ATCC (listed as ATCC-VR1616 and ATCC-VR1816, respectively). Their respective  
267 titers provided by ARMWG are  $3.28 \times 10^{10}$  GC/ml and  $5.75 \times 10^{11}$  GC/ml<sup>38, 41</sup>. We  
268 decided to use AAV8RSM for validation because its titer is higher and also because it  
269 has been extensively characterized. Many details were included in a series of  
270 publications<sup>26, 32, 38, 42</sup>, making it possible to compare our data with the literature values.

271 To measure the titer of AAV8RSM, we conducted three independent assays, with  
272 each assay performed in triplicates. For lysed samples, 1  $\mu$ l of AAV8RSM was diluted in

273 10 ul PBS, followed by 2  $\mu$ l of NaOH (500 mM) treatment for 2 minutes and then 2 ul of  
274 Tris (1M, PH 5.0) neutralization. For unlysed controls, 1  $\mu$ l of AAV8RSM was simply  
275 diluted in PBS without addition of NaOH and Tris buffer. 12-point DNA standards  
276 ranging from 0 to 5.0 ng were also prepared. DNA binding assay was conducted as  
277 described before. Data from all three experiments was summarized in table 1.

278 An example to illustrate the analysis process is provided in Figure 4. In this  
279 experiment, unlysed samples exhibited fluorescence ( $527.5 \pm 12.5$ , n=3) similar to  
280 sample blanks ( $516.8 \pm 22.3$ , n=3), indicating that contamination of non-encapsided  
281 DNA was low in AAV8RSM. Based on the standard curve (Figure 4, inset), we  
282 estimated non-encapsided DNA to be 0.15 ng for each ul of AAV8RSM. Meanwhile  
283 lysed samples exhibited averaged fluorescence of  $762.7 \pm 27.42$  (n=3), translating to  
284 1.20 ng of DNA per ul of AAV8RSM. Therefore, encapsided DNA, calculated by  
285 subtracting values of unlysed samples from value of lysed samples, equals to 1.05 ng/  
286 ul virus. Based on the provided equation, titer of AAV8RSM from this experiment was  
287 calculated to be  $4.7 \times 10^{11}$  GC/ml.

288 In the same way we calculated titers of AAV8RSM for each independent assay  
289 (Table 1). At first glance, titers determined in each replicate, from all three experiments,  
290 fall into the range of  $3-5 \times 10^{11}$  GC/ml, similar to those obtained by Elisa method in  
291 previous studies<sup>26, 32, 38, 42</sup>. We will discuss this in more details in the discussion section.  
292 Intra-assay analysis was performed and it revealed low coefficients of variation (CV),  
293 with the highest being 16.4% and lowest being 7.7% (Table 1). Inter-assay analysis of  
294 three independent experiments showed mean titer of  $4.23 \times 10^{11}$ , with low 95%  
295 confidence interval (CI) and high 95% CI to be  $2.50 \times 10^{11}$  and  $5.97 \times 10^{11}$  respectively,  
296 and with inter-assay CV to be 16.3%. Taken together, coefficients of variation of both

297 inter-assay and intra-assay are quite low, indicating high repeatability and reproducibility  
298 of the GelGreen method (Table 1).

299

### 300 **Evaluation of the accuracy of GelGreen® - based AAV titration method**

301 To further evaluate accuracy of the GelGreen method, we designed and  
302 performed a new experiment, in which we adopted the concept of amplification  
303 efficiency from qPCR analysis. The amplification efficiency of qPCR is calculated as  $E =$   
304  $-1 + n^{(-1/\text{slope})}$  where  $n$  is dilution factor and slope can be derived from linear regression of  
305 threshold cycle (Ct) vs. log of input DNA. In general, efficiency between 90% and 110%  
306 is acceptable.

307 In a similar way, we measured efficiency of GelGreen method using serial 2-fold  
308 dilution of a home-made rAAV sample. We used NaOH to lyse viral particles and  
309 conducted DNA quantification as before. DNA standard curve is shown in Figure 5A.  
310 As expected, fluorescence of serially diluted AAV samples progressively declined  
311 (Figure 5B). Similarly, DNA mass, which was converted from fluorescence based on  
312 standard curve, also took steps down during serial dilution (Figure 5C). We recognized  
313 that 1  $\mu\text{l}$  of viral sample contained  $\sim 18$  ng DNA. A simple calculation yielded a titer of  
314  $6.99 \times 10^{12}$  for this sample (Figure 5C). After six rounds of two-fold dilution, total DNA  
315 was reduced to less than 0.3 ng and consequently became non-detectable (Figure 5 B-  
316 D). Meanwhile, linear relationships existed between  $\text{Log}_2(\text{DNA})$  and number of dilutions  
317 up to 6 (Figure 1D). Slopes from three independent serial dilutions were derived from  
318 the linear portion of the curves to attain a mean value of  $-0.96 \pm 0.04$ . Accordingly, we  
319 calculated efficiency of GelGreen method to be  $106 \pm 11$  %, which is very close to the  
320 theoretical 100% efficiency.

## 321 **Visualization of rAAV quantity with gel imager**

322 Having measured AAV titer with plate reader, we wondered if we can even  
323 “visualize” AAV titer directly with a gel imager. We are equipped with a system intended  
324 for imaging ethidium bromide (EB) stained DNA. Thus we chose GelRed® in this  
325 experiment because its fluorescence properties are similar to that of EB. A pilot  
326 experiment found that 1/10 000 dilution of GelRed® is also the optimal dilution factor for  
327 DNA detection, like GelGreen®.

328 We selected a rAAV sample whose titer was about  $4.5 \times 10^{12}$ . We made four-  
329 point serial dilution (2-fold) of virus in a PCR strip, with the starting tube containing 1  $\mu$ l  
330 virus diluted in 10  $\mu$ l of PBS. Samples were heated at 95 °C for 5 minutes in a PCR  
331 thermo-cycler. After heating, we pipetted 5  $\mu$ l of 1/3,300 GelRed® into PCR strip to  
332 make final 1/10 000 GelRed® dilution. We also made DNA standard (0-50 ng) in a PCR  
333 strip. Viral samples and DNA standard were imaged simultaneously with gel imager  
334 (Figure 6A). By side-by-side comparison, it is quite easy to approximate that the amount  
335 of DNA in the starting tube is between 6.26 to 12.5 ng. To be more quantitative, we  
336 analyzed image file with image J software to generate a calibration plot. This plot shows  
337 linear relationship between fluorescence intensity and DNA up to 25 ng (Figure 6B).  
338 Based on the standard curve, we calculated the DNA content in the starting tube to be  
339 11.9 ng. Similarly, viral sample’s DNA contents at each dilution were derived. The plot  
340 of  $\text{Log}_2(\text{DNA})$  vs dilution showed a linear relationship with a slope of -0.87, which  
341 yielded a 121% efficiency (Figure 6C). Thus, simple imaging method provided a quick,  
342 and fairly effective way to estimate AAV titers.

343

## 344 **Discussion**

345 Here we report a method to quantify AAV vectors based on binding of AAV's  
346 DNA with a safe nucleic dye. This method offers several advantages. First, it is very  
347 fast. It allows determination of AAV titrations in about 30 minutes. Second, it is safe and  
348 cost-efficient. The Biotum dyes we used are membrane impermeant, making them safer  
349 to use and less hazardous to environment. It is also economical. Each experiment  
350 typically requires less than 1  $\mu$ l of dye, costing only 20-30 cents. Most importantly, this  
351 method is consistent, as inter-assay and intra-assay variations are both small. We  
352 believe this is mainly due to the fact that DNA was measured directly without  
353 amplification. Skipping amplification steps makes the assay less sensitive to many  
354 factors that are crucial for enzyme-based reactions, such as PCR and capsid Elisa. The  
355 main disadvantage of the method is its low sensitivity, at least when compared to qPCR  
356 method and Elisa. Since LOD of GelGreen is  $\sim 0.3$  ng, we estimate that the lowest AAV  
357 titer this method can detect is about  $1.0 \times 10^{10}$  gc/ml at the expense of 10  $\mu$ l of viral  
358 sample.

359 AAV genome is single-stranded DNA (ssDNA) of approximately 4.7-kilobases  
360 (kb). It was flanked with two 145 nucleotide-long inverted terminal repeats (ITR) that  
361 actually form double stranded DNA (dsDNA). Thus in its natural form, AAV genome is  
362 made of both ssDNA and dsDNA. Although it has been suggested that following  
363 denaturation AAV genome anneals to form dsDNA<sup>18</sup>, the extent to which dsDNA is  
364 converted from ssDNA remains unclear. Given this concern, it is perhaps less  
365 compelling to use exclusive dsDNA dyes such as CyQuant and picoGreen for AAV  
366 titration. On the other hand, GelRed® and GelGreen® dyes bind both ssDNA and  
367 dsDNA, making them more suitable than dsDNA dyes for measuring AAV's genome  
368 content.



369 We have explored two methods for releasing viral DNA from viral particles. The  
370 first method is heat inactivation. It has been demonstrated that AAV serotypes are  
371 different in their thermal stability, with rAAV2 being the least thermal stable and rAAV5  
372 being the most thermal stable. In PBS buffer, the melting temperature ( $T_m$ s) of different  
373 AAV serotypes range from 66.5 up to 89.5 °C<sup>43</sup>. Therefore we choose to heat rAAV  
374 samples at 95 °C. At such high temperature, even the most stable rAAV5 should be  
375 destroyed. The second method we used is the alkaline lysis method. In our experiment,  
376 we found the  $EC_{50}$  of NaOH treatment to be 12 mM for AAV serotype 2. It remains to be  
377 examined whether different AAV serotypes share a similar sensitivity to NaOH  
378 treatment. To be more rigorous, we have used high concentration of NaOH (100 mM) in  
379 our experiments to lyse AAV.

380 AAV8RSM has been extensively characterized by ARMWG. In the first paper  
381 published in 2014<sup>38</sup>, genome titer was determined be  $9.62 \times 10^{11}$  GC/ml, based on  
382 qPCR data obtained from 16 labs. However, significant variations were found among  
383 these labs, with almost 100-fold difference between the lowest titer ( $4.6 \times 10^{10}$  GC/ml)  
384 and the highest titer ( $4.7 \times 10^{12}$  GC/ml). Elisa method was also used to measure capsid  
385 particle titer of AAV8RSM. This assay yielded a value of  $5.5 \times 10^{11}$ , which is actually  
386 lower than the value determined by qPCR<sup>38</sup>. The second paper published in 2016  
387 demonstrated a “free-ITR” qPCR method. Using this method, the titer of AAV8RSM was  
388 measured to be  $5.65 \times 10^{11}$  GC/ml, which was close to the titer determined by dot blot  
389 method and Elisa methods (Table 4, D’Costa et al.<sup>26</sup>). In the third paper published in  
390 2018, AAV8RSM titer was determined to be  $5.65 \times 10^{11}$  GC/ml by qPCR targeting the  
391 SV40 polyA sequence (Table 1, François et al.<sup>42</sup>). This result is similar to the results  
392 published in 2016<sup>26</sup>. However in 2019, three independent labs from ARMWG carried out

393 AAV8RSM titration again<sup>32</sup>. This time, the genome titer determined by qPCR ( $1.48 \pm$   
394  $0.618 \times 10^{12}$  GC/m) was 2-3 fold higher than total capsid particle titer determined by  
395 Elisa ( $5.76 \pm 0.33 \times 10^{11}$ ). So despite a series of studies that spanned many years,  
396 discrepancies remain to be resolved, although it was evident that ELISA method was  
397 more consistent than qPCR method<sup>32</sup>.

398 We decided to statistically compare the titer determined by GelGreen method in  
399 our study to the titers determined by Elisa and qPCR methods in ARMWG's most recent  
400 report<sup>32</sup>. For this purpose, we imported results from Penaud-Budloo et al.<sup>32</sup> and re-  
401 plotted their data as "Elisa" group and "qPCR" group in parallel with our GelGreen data  
402 (Figure 7). One-way ANOVA revealed significant difference among the three groups  
403 ( $F_{2,7} = 6.053$ ,  $p < 0.05$ ). Tukey's post-test showed that the GelGreen group is significantly  
404 different from the qPCR group but is not different from the Elisa group. Specifically, titer  
405 measured by GelGreen was  $4.23 \pm 0.70 \times 10^{11}$ , which is slightly lower although is still  
406 within one standard deviation to the titer measured by capsid ELISA ( $5.73 \pm 2.62$   
407  $\times 10^{11}$ ).

408 In conclusion, we report a protocol to measure AAV titer using safe nucleic acid  
409 dyes. This protocol is simple, safe, reliable and cost-efficient. It could be broadly applied  
410 for quantification and normalization of AAV vectors. Future studies can explore more  
411 DNA dyes and may find improvements in detection limit.

## 412 **Acknowledgements**

413 The authors thank Northwestern University Analytical BioNanotechnology Equipment  
414 Core facility of the Simpson Querrey Institute for providing Cytation 3 plate readers and  
415 for technical support.

416

## 417 **Conflict of Interest**

418 The authors declare that they have no conflict of interest.

419

## 420 **Author Contributions & Funding Sources**

421 JX , YZ and SHD designed experiments, collected and analyzed data, and wrote the  
422 manuscript. This work was supported by NIH R01 EY030169 to YZ, Whitehall grant to  
423 YZ and NIH R01 EY018204 to SHD.

## 424 **Figure legends**

### 425 **Figure 1. Detection of DNA by GelGreen®.**

426 (A) Calibration plot of fluorescence intensity vs. DNA. Each line represents different  
427 dilutions of GelGreen®. Between 1/3000 to 1/100 000 dilution, GelGreen® showed  
428 linearity for DNA in the range of 0-50 ng. Results are averaged from triplicate wells.  
429 Bars indicate SD.

430 (B) Plot of fluorescence intensity vs. DNA in logarithmic x-axis and y-axis. Each line  
431 represents different dilutions of GelGreen®. Results are averaged from triplicate wells.  
432 Bars indicate SD.

433 (C) Effects of dye concentrations. Each line represents different amount of DNA. The  
434 results are averaged from triplicate samples. Bars indicate SD.

435 (D) Limit of detection and quantification. GelGreen® was at 1/10 000. The plot shows an  
436 enlarged scale for DNA < 4 ng. Results are averaged from triplicate wells. Bars indicate  
437 SD. Limit of detection (LOD) (0.19 ng) and limit of quantification (LOQ) (0.35 ng) are  
438 marked with dashed lines. \*\* indicates statistically significant difference (t-test,  $p < 0.01$ )  
439 compared to blanks (0 ng).

440

### 441 **Figure 2. Release of viral DNA by heating at 95 °C.**

442 (A) Time course of fluorescence intensity during heating. Each line represents different  
443 concentration of SDS. Results are averaged from triplicate samples. Bars indicate SD.

444 (B) Effects of SDS on DNA binding assay. Shown are series of curves of fluorescence  
445 vs DNA, with DNA ranging from 0-50 ng. Each curve represents different concentration  
446 of SDS. Results are averaged from triplicate wells. Bars indicate SD.

447

448 **Figure 3. Release of viral DNA by alkaline lysis.**

449 (A) Fluorescence changes in response to NaOH treatment. NaOH ranges from 0 to 250  
450 mM. Results are averaged from triplicate samples. Bars indicate SD.

451 (B) Effects of combining alkaline lysis and heating procedures on viral lysis. Results are  
452 averaged from triplicate samples. Bars indicate SD. ns = not significant.

453

454 **Figure 4. Titration of AAV8RSM by GelGreen method.**

455 (A) Calibration plot of standard DNA in linear-linear scale and in log-log scale (inset).

456 The DNA standard was made by serial dilution from 5 ng with dilution effect of 0.7.

457 Trend lines, linear regression equations and  $R^2$  are shown. Dash lines are for three

458 untreated rAAV sample intersecting Y-axis at 514, 529 and 539 (green), and three

459 NaOH-treated samples at Y-axis of 771, 732 and 781 (red) respectively.

460

461 **Figure 5. Evaluation of the accuracy of the GelGreen-based AAV titration method.**

462 (A) DNA standard curve (log-log plot). DNA standard was made by two-fold serial  
463 dilution, ranging from 0 to 50 ng. Red circles on the fitted line indicate fluorescence of  
464 AAV virus (averaged from triplicate samples) at different dilutions.

465 (B) Fluorescence of serially diluted AAV virus. Results are averaged from triplicate  
466 samples. Bars indicate SD.

467 (C) Plot of converted viral DNA mass vs. dilutions. Results are averaged from triplicate  
468 samples. Bars indicate SD.

469 (D) Plot of  $\text{Log}_2$  of the DNA vs. dilutions. Each line represents one dilution series ( $n=3$ ).

470 Linear relationships exist when the dilution rounds were less than 6. Trend lines, linear

471 regression equations and  $R^2$  are shown.

472

473 **Figure 6. Direct visualization of quantities of rAAV using gel imager.**

474 (A) Images of DNA standard (top) and AAV samples (Bottom) stained by 1/10 000

475 GelRed®. DNA standard was made by two-fold serial dilution, starting at 50 ng. AAV

476 samples consisted of 4-point twofold dilution series.

477 (B) Calibration plot of DNA standard. GelRed® shows linearity for the range of 0-25 ng

478 DNA. Trend lines, linear regression equations and  $R^2$  are shown. Red circles on the

479 fitted line indicate fluorescence of serially diluted vial samples.

480 (C) Linear approximation of Log<sub>2</sub> DNA input vs. dilution. Calculated slope and  $R^2$  are

481 shown.

482

483 **Figure 7. Comparisons of titers of AAV8RSM determined by different methods.**

484 Bar graph showing titers of AAV8RSM determined by three different methods. The first

485 set of data is based on GelGreen method in this study. The second set (Elisa) and third

486 set (qPCR) of data was imported directly from Table 3 and Table 1 of Penaud-Budloo

487 2019<sup>32</sup>. Bars indicate SD. #,  $p < 0.05$ , one way ANOVA; \*,  $p < 0.05$ , Tukey multi-

488 comparison test.

489

## 490 References

- 491 1. Wang D, Tai PWL, Gao G. Adeno-associated virus vector as a platform for gene  
492 therapy delivery. *Nature reviews. Drug discovery* 2019; **18**(5): 358-378.  
493
- 494 2. Zinn E, Vandenberghe LH. Adeno-associated virus: fit to serve. *Current opinion in*  
495 *virology* 2014; **8**: 90-7.  
496
- 497 3. Betley JN, Sternson SM. Adeno-associated viral vectors for mapping, monitoring, and  
498 manipulating neural circuits. *Human gene therapy* 2011; **22**(6): 669-77.  
499
- 500 4. Hermonat PL, Muzyczka N. Use of adeno-associated virus as a mammalian DNA  
501 cloning vector: transduction of neomycin resistance into mammalian tissue culture  
502 cells. *Proceedings of the National Academy of Sciences of the United States of America*  
503 1984; **81**(20): 6466-70.  
504
- 505 5. Kaplitt MG, Leone P, Samulski RJ, Xiao X, Pfaff DW, O'Malley KL *et al.* Long-term gene  
506 expression and phenotypic correction using adeno-associated virus vectors in the  
507 mammalian brain. *Nature genetics* 1994; **8**(2): 148-54.  
508
- 509 6. Day TP, Byrne LC, Schaffer DV, Flannery JG. Advances in AAV vector development for  
510 gene therapy in the retina. *Advances in experimental medicine and biology* 2014;  
511 **801**: 687-93.  
512
- 513 7. Flotte T, Carter B, Conrad C, Guggino W, Reynolds T, Rosenstein B *et al.* A phase I  
514 study of an adeno-associated virus-CFTR gene vector in adult CF patients with mild  
515 lung disease. *Human gene therapy* 1996; **7**(9): 1145-59.  
516
- 517 8. Bennicelli J, Wright JF, Komaromy A, Jacobs JB, Hauck B, Zelenia O *et al.* Reversal of  
518 blindness in animal models of leber congenital amaurosis using optimized AAV2-  
519 mediated gene transfer. *Molecular therapy : the journal of the American Society of*  
520 *Gene Therapy* 2008; **16**(3): 458-65.  
521
- 522 9. Cideciyan AV, Aleman TS, Boye SL, Schwartz SB, Kaushal S, Roman AJ *et al.* Human  
523 gene therapy for RPE65 isomerase deficiency activates the retinoid cycle of vision  
524 but with slow rod kinetics. *Proceedings of the National Academy of Sciences of the*  
525 *United States of America* 2008; **105**(39): 15112-7.  
526
- 527 10. Hauswirth WW, Aleman TS, Kaushal S, Cideciyan AV, Schwartz SB, Wang L *et al.*  
528 Treatment of leber congenital amaurosis due to RPE65 mutations by ocular  
529 subretinal injection of adeno-associated virus gene vector: short-term results of a  
530 phase I trial. *Human gene therapy* 2008; **19**(10): 979-90.  
531
- 532 11. Samulski RJ, Chang LS, Shenk T. Helper-free stocks of recombinant adeno-associated  
533 viruses: normal integration does not require viral gene expression. *Journal of*  
534 *virology* 1989; **63**(9): 3822-8.  
535

- 536 12. Sondhi D, Peterson DA, Giannaris EL, Sanders CT, Mendez BS, De B *et al.* AAV2-  
537 mediated CLN2 gene transfer to rodent and non-human primate brain results in  
538 long-term TPP-I expression compatible with therapy for LINCL. *Gene therapy* 2005;  
539 **12**(22): 1618-32.  
540
- 541 13. Grimm D, Kern A, Pawlita M, Ferrari F, Samulski R, Kleinschmidt J. Titration of AAV-  
542 2 particles via a novel capsid ELISA: packaging of genomes can limit production of  
543 recombinant AAV-2. *Gene therapy* 1999; **6**(7): 1322-30.  
544
- 545 14. Zeltner N, Kohlbrenner E, Clement N, Weber T, Linden RM. Near-perfect infectivity  
546 of wild-type AAV as benchmark for infectivity of recombinant AAV vectors. *Gene*  
547 *therapy* 2010; **17**(7): 872-9.  
548
- 549 15. Aurnhammer C, Haase M, Muether N, Hausl M, Rauschhuber C, Huber I *et al.*  
550 Universal real-time PCR for the detection and quantification of adeno-associated  
551 virus serotype 2-derived inverted terminal repeat sequences. *Human gene therapy*  
552 *methods* 2012; **23**(1): 18-28.  
553
- 554 16. Grieger JC, Choi VW, Samulski RJ. Production and characterization of adeno-  
555 associated viral vectors. *Nature protocols* 2006; **1**(3): 1412-28.  
556
- 557 17. Veldwijk MR, Topaly J, Laufs S, Hengge UR, Wenz F, Zeller WJ *et al.* Development and  
558 optimization of a real-time quantitative PCR-based method for the titration of AAV-2  
559 vector stocks. *Molecular therapy : the journal of the American Society of Gene Therapy*  
560 2002; **6**(2): 272-8.  
561
- 562 18. Sommer JM, Smith PH, Parthasarathy S, Isaacs J, Vijay S, Kieran J *et al.* Quantification  
563 of adeno-associated virus particles and empty capsids by optical density  
564 measurement. *Molecular therapy : the journal of the American Society of Gene*  
565 *Therapy* 2003; **7**(1): 122-8.  
566
- 567 19. Piedra J, Ontiveros M, Miravet S, Penalva C, Monfar M, Chillon M. Development of a  
568 rapid, robust, and universal picogreen-based method to titer adeno-associated  
569 vectors. *Human gene therapy methods* 2015; **26**(1): 35-42.  
570
- 571 20. Kohlbrenner E, Henckaerts E, Rapti K, Gordon RE, Linden RM, Hajjar RJ *et al.*  
572 Quantification of AAV particle titers by infrared fluorescence scanning of coomassie-  
573 stained sodium dodecyl sulfate-polyacrylamide gels. *Human gene therapy methods*  
574 2012; **23**(3): 198-203.  
575
- 576 21. Ayuso E, Mingozzi F, Montane J, Leon X, Anguela XM, Haurigot V *et al.* High AAV  
577 vector purity results in serotype- and tissue-independent enhancement of  
578 transduction efficiency. *Gene therapy* 2010; **17**(4): 503-10.  
579
- 580 22. Zen Z, Espinoza Y, Bleu T, Sommer JM, Wright JF. Infectious titer assay for adeno-  
581 associated virus vectors with sensitivity sufficient to detect single infectious events.  
582 *Human gene therapy* 2004; **15**(7): 709-15.



- 583  
584 23. Salvetti A, Oreve S, Chadeuf G, Favre D, Cherel Y, Champion-Arnaud P *et al.* Factors  
585 influencing recombinant adeno-associated virus production. *Human gene therapy*  
586 1998; **9**(5): 695-706.  
587
- 588 24. Mohiuddin I, Loiler S, Zolotukhin I, Byrne BJ, Flotte TR, Snyder RO. Herpesvirus-  
589 based infectious titering of recombinant adeno-associated viral vectors. *Molecular*  
590 *therapy : the journal of the American Society of Gene Therapy* 2005; **11**(2): 320-6.  
591
- 592 25. Werling NJ, Satkunanathan S, Thorpe R, Zhao Y. Systematic Comparison and  
593 Validation of Quantitative Real-Time PCR Methods for the Quantitation of Adeno-  
594 Associated Viral Products. *Human gene therapy methods* 2015; **26**(3): 82-92.  
595
- 596 26. D'Costa S, Blouin V, Broucque F, Penaud-Budloo M, Francois A, Perez IC *et al.*  
597 Practical utilization of recombinant AAV vector reference standards: focus on vector  
598 genomes titration by free ITR qPCR. *Molecular therapy. Methods & clinical*  
599 *development* 2016; **5**: 16019.  
600
- 601 27. Lock M, Alvira MR, Chen SJ, Wilson JM. Absolute determination of single-stranded  
602 and self-complementary adeno-associated viral vector genome titers by droplet  
603 digital PCR. *Human gene therapy methods* 2014; **25**(2): 115-25.  
604
- 605 28. Dobnik D, Kogovsek P, Jakomin T, Kosir N, Tusek Znidaric M, Leskovec M *et al.*  
606 Accurate Quantification and Characterization of Adeno-Associated Viral Vectors.  
607 *Frontiers in microbiology* 2019; **10**: 1570.  
608
- 609 29. Jones LJ, Gray M, Yue ST, Haugland RP, Singer VL. Sensitive determination of cell  
610 number using the CyQUANT cell proliferation assay. *Journal of immunological*  
611 *methods* 2001; **254**(1-2): 85-98.  
612
- 613 30. Dragan AI, Casas-Finet JR, Bishop ES, Strouse RJ, Schenerman MA, Geddes CD.  
614 Characterization of PicoGreen interaction with dsDNA and the origin of its  
615 fluorescence enhancement upon binding. *Biophysical journal* 2010; **99**(9): 3010-9.  
616
- 617 31. Ahn SJ, Costa J, Emanuel JR. PicoGreen quantitation of DNA: effective evaluation of  
618 samples pre- or post-PCR. *Nucleic acids research* 1996; **24**(13): 2623-5.  
619
- 620 32. Penaud-Budloo M, Broucque F, Harrouet K, Bouzelha M, Saleun S, Douthe S *et al.*  
621 Stability of the adeno-associated virus 8 reference standard material. *Gene therapy*  
622 2019; **26**(5): 211-215.  
623
- 624 33. Samulski RJ, Muzyczka N. AAV-Mediated Gene Therapy for Research and  
625 Therapeutic Purposes. *Annual review of virology* 2014; **1**(1): 427-51.  
626
- 627 34. Xiao X, Li J, Samulski RJ. Production of high-titer recombinant adeno-associated  
628 virus vectors in the absence of helper adenovirus. *Journal of virology* 1998; **72**(3):  
629 2224-32.

- 630  
631 35. Zhu Y, Xu J, Hauswirth WW, DeVries SH. Genetically targeted binary labeling of  
632 retinal neurons. *The Journal of neuroscience : the official journal of the Society for*  
633 *Neuroscience* 2014; **34**(23): 7845-61.  
634
- 635 36. Jara JH, Stanford MJ, Zhu Y, Tu M, Hauswirth WW, Bohn MC *et al.* Healthy and  
636 diseased corticospinal motor neurons are selectively transduced upon direct AAV2-  
637 2 injection into the motor cortex. *Gene therapy* 2016; **23**(3): 272-82.  
638
- 639 37. Zolotukhin S, Byrne BJ, Mason E, Zolotukhin I, Potter M, Chesnut K *et al.*  
640 Recombinant adeno-associated virus purification using novel methods improves  
641 infectious titer and yield. *Gene therapy* 1999; **6**(6): 973-85.  
642
- 643 38. Ayuso E, Blouin V, Lock M, McGorray S, Leon X, Alvira MR *et al.* Manufacturing and  
644 characterization of a recombinant adeno-associated virus type 8 reference standard  
645 material. *Human gene therapy* 2014; **25**(11): 977-87.  
646
- 647 39. Xu J, Zhu Y. A rapid in vitro method to flip back the double-floxed inverted open  
648 reading frame in a plasmid. *BMC biotechnology* 2018; **18**(1): 52.  
649
- 650 40. Burger C, Gorbatyuk OS, Velardo MJ, Peden CS, Williams P, Zolotukhin S *et al.*  
651 Recombinant AAV viral vectors pseudotyped with viral capsids from serotypes 1, 2,  
652 and 5 display differential efficiency and cell tropism after delivery to different  
653 regions of the central nervous system. *Molecular therapy : the journal of the*  
654 *American Society of Gene Therapy* 2004; **10**(2): 302-17.  
655
- 656 41. Lock M, McGorray S, Auricchio A, Ayuso E, Beecham EJ, Blouin-Tavel V *et al.*  
657 Characterization of a recombinant adeno-associated virus type 2 Reference  
658 Standard Material. *Human gene therapy* 2010; **21**(10): 1273-85.  
659
- 660 42. Francois A, Bouzelha M, Lecomte E, Broucque F, Penaud-Budloo M, Adjali O *et al.*  
661 Accurate Titration of Infectious AAV Particles Requires Measurement of Biologically  
662 Active Vector Genomes and Suitable Controls. *Molecular therapy. Methods & clinical*  
663 *development* 2018; **10**: 223-236.  
664
- 665 43. Bennett A, Patel S, Mietzsch M, Jose A, Lins-Austin B, Yu JC *et al.* Thermal Stability as  
666 a Determinant of AAV Serotype Identity. *Molecular therapy. Methods & clinical*  
667 *development* 2017; **6**: 171-182.  
668  
669

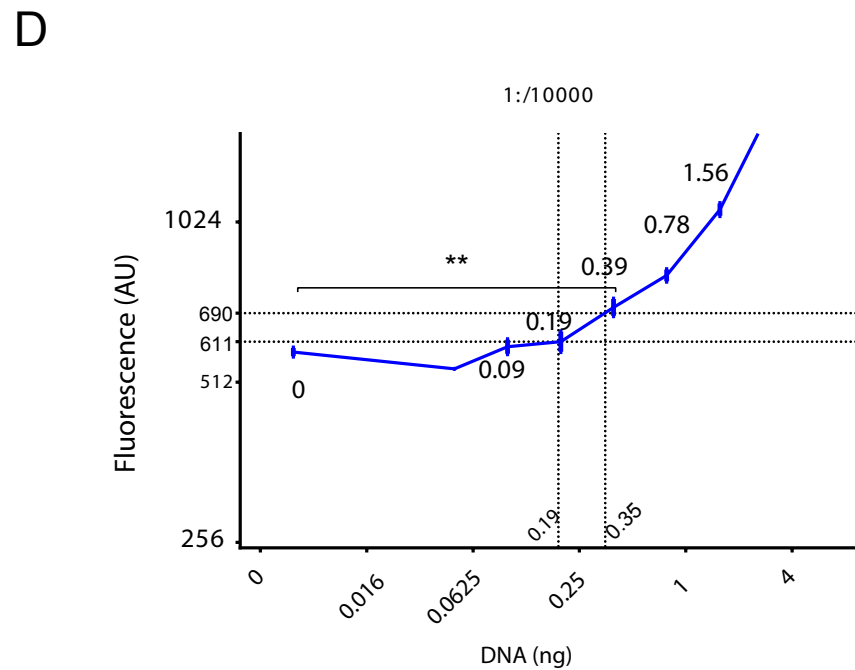
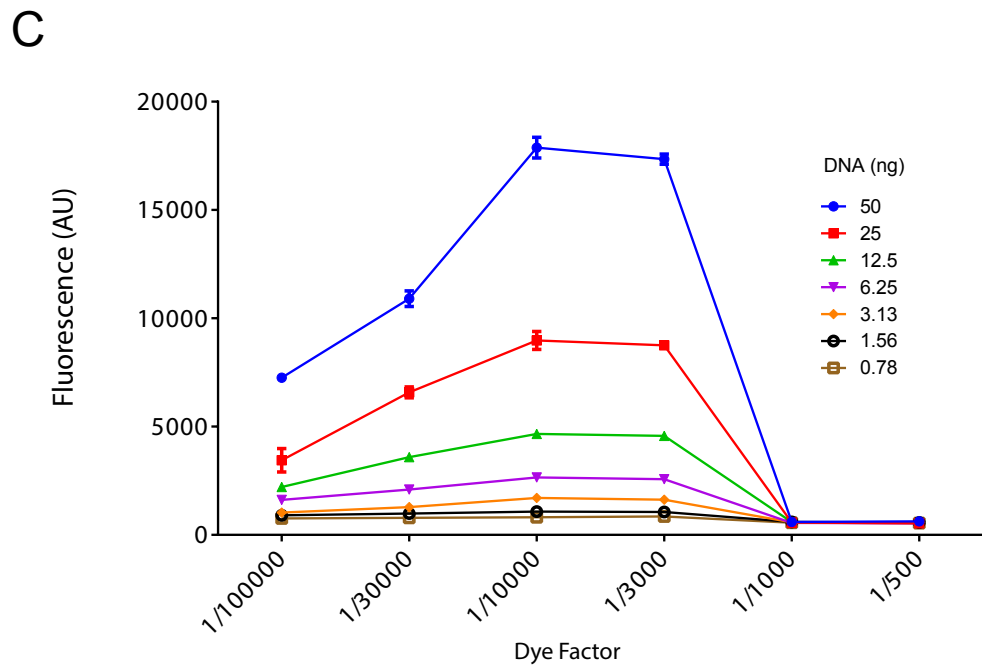
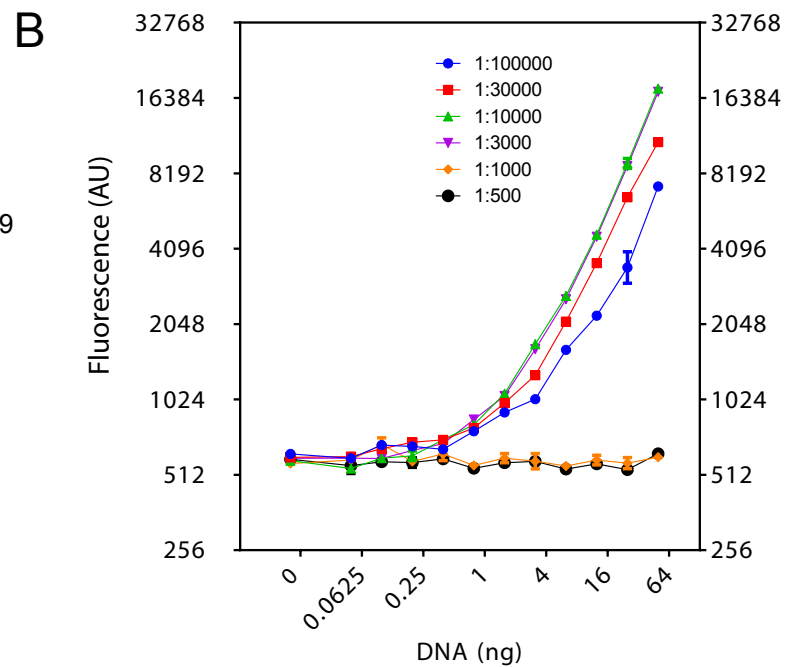
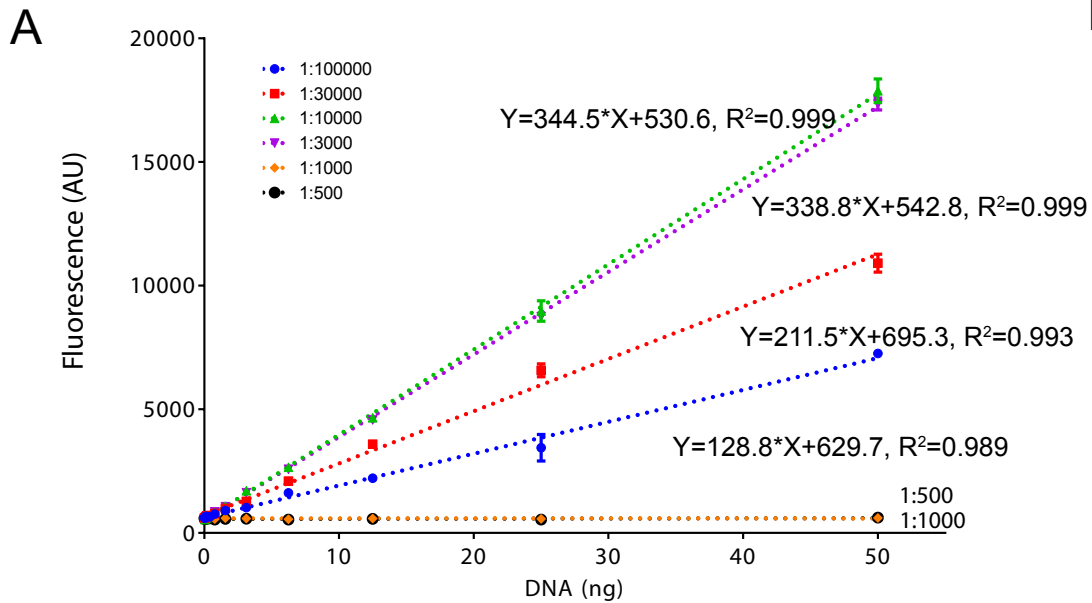
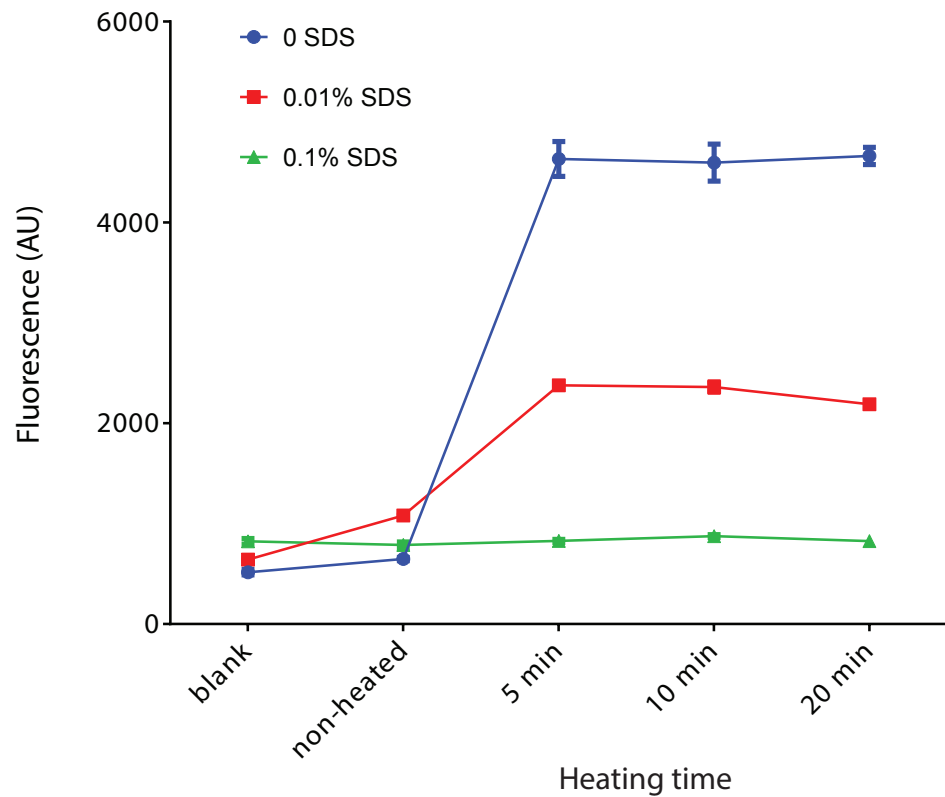


Figure 1

A



B

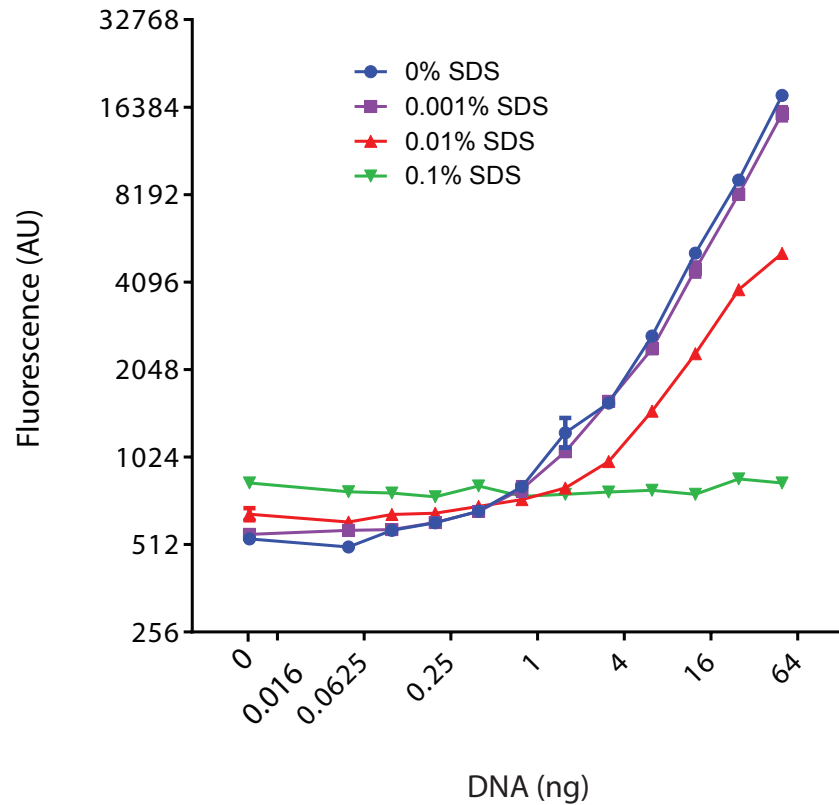
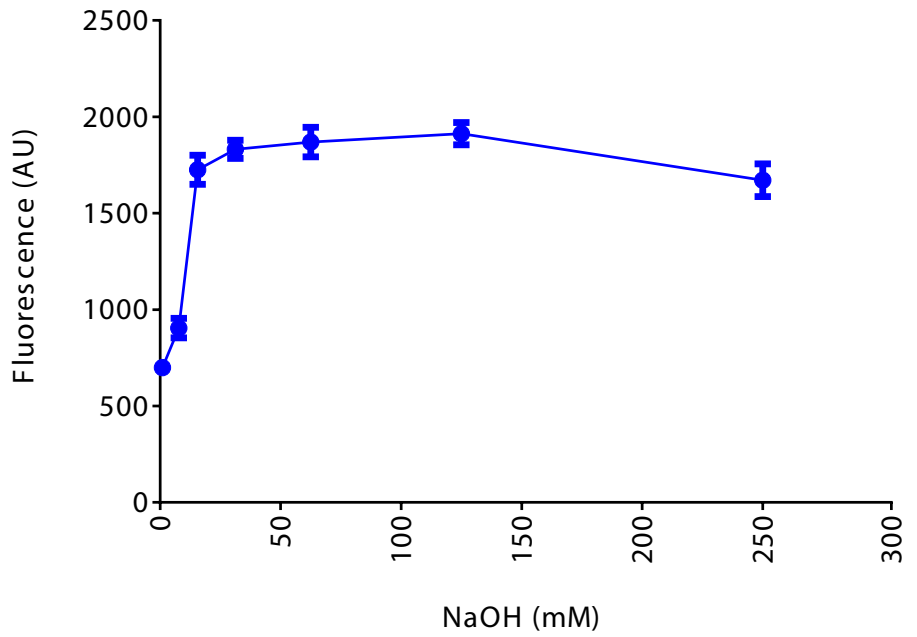
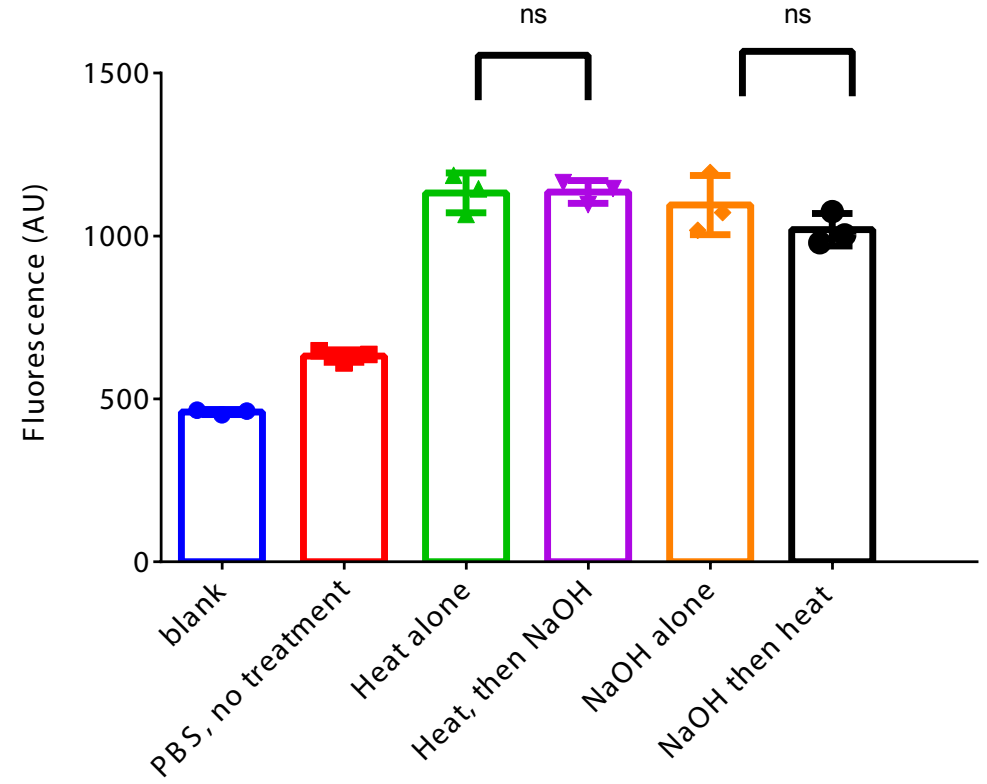


Figure 2

**A****B****Figure 3**

A

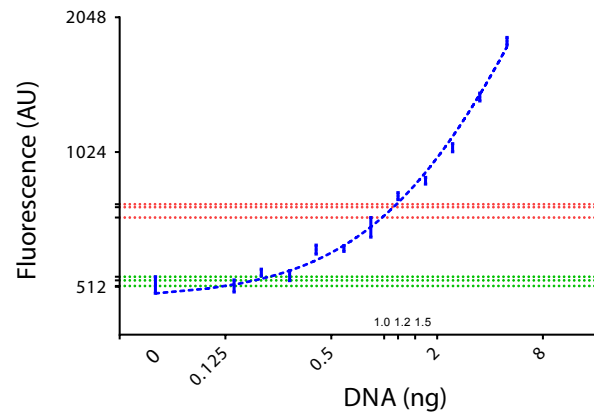
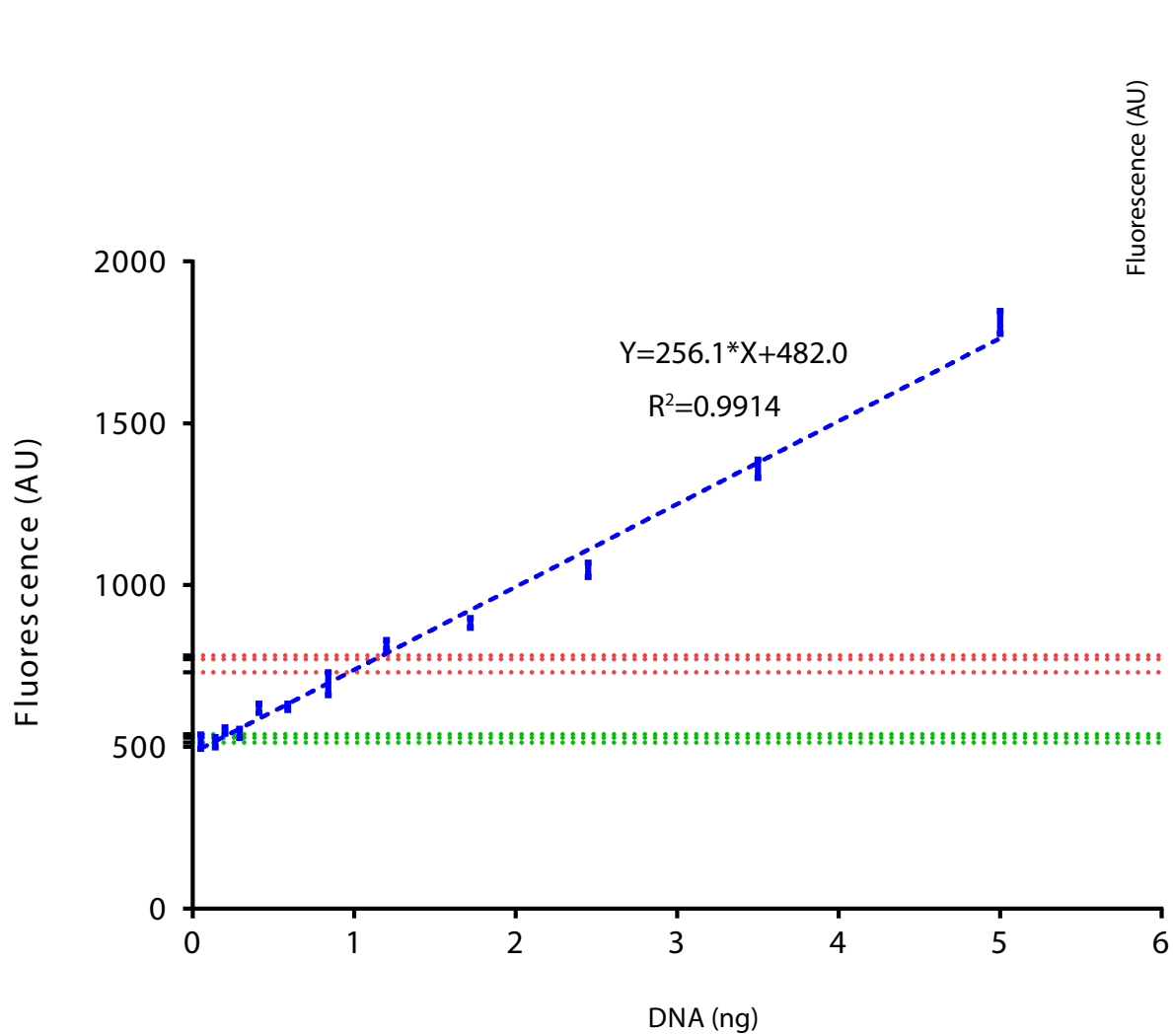


Figure 4

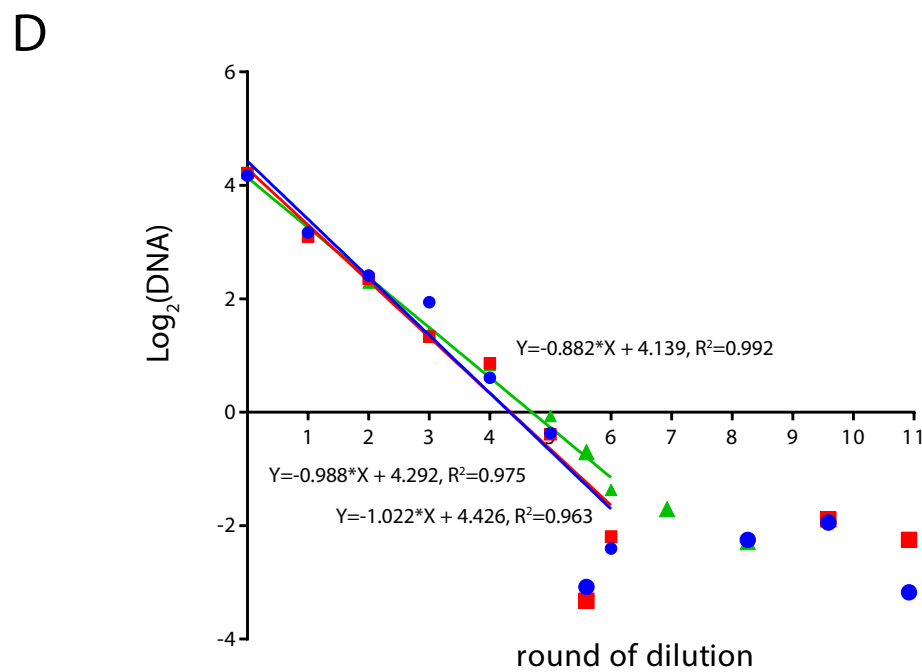
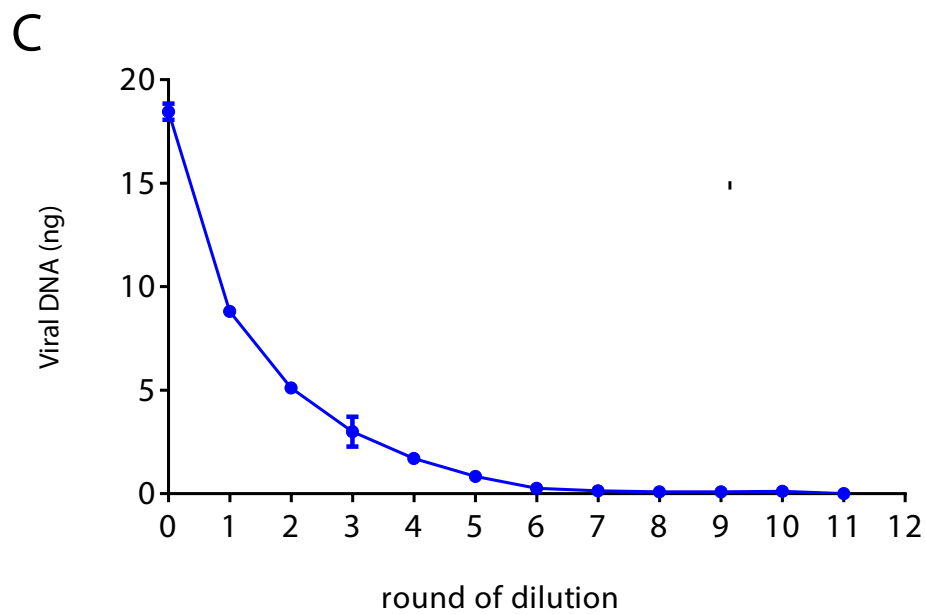
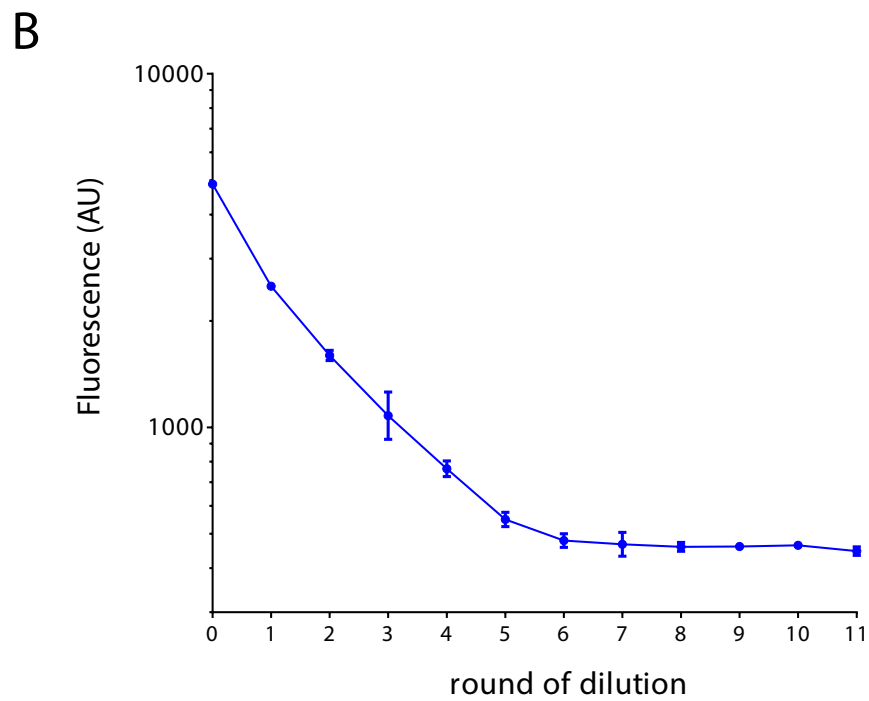
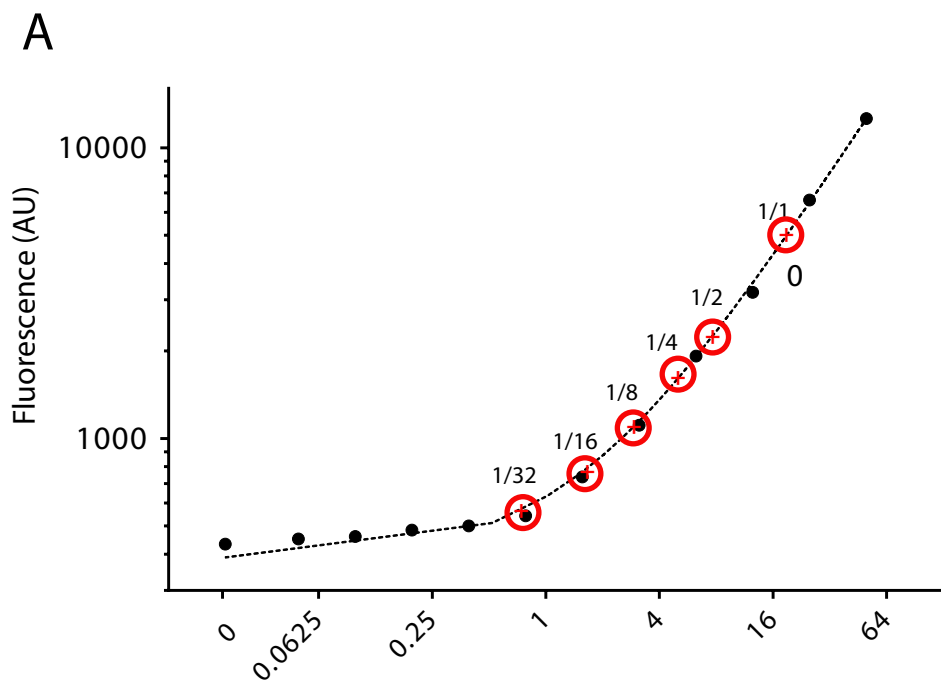
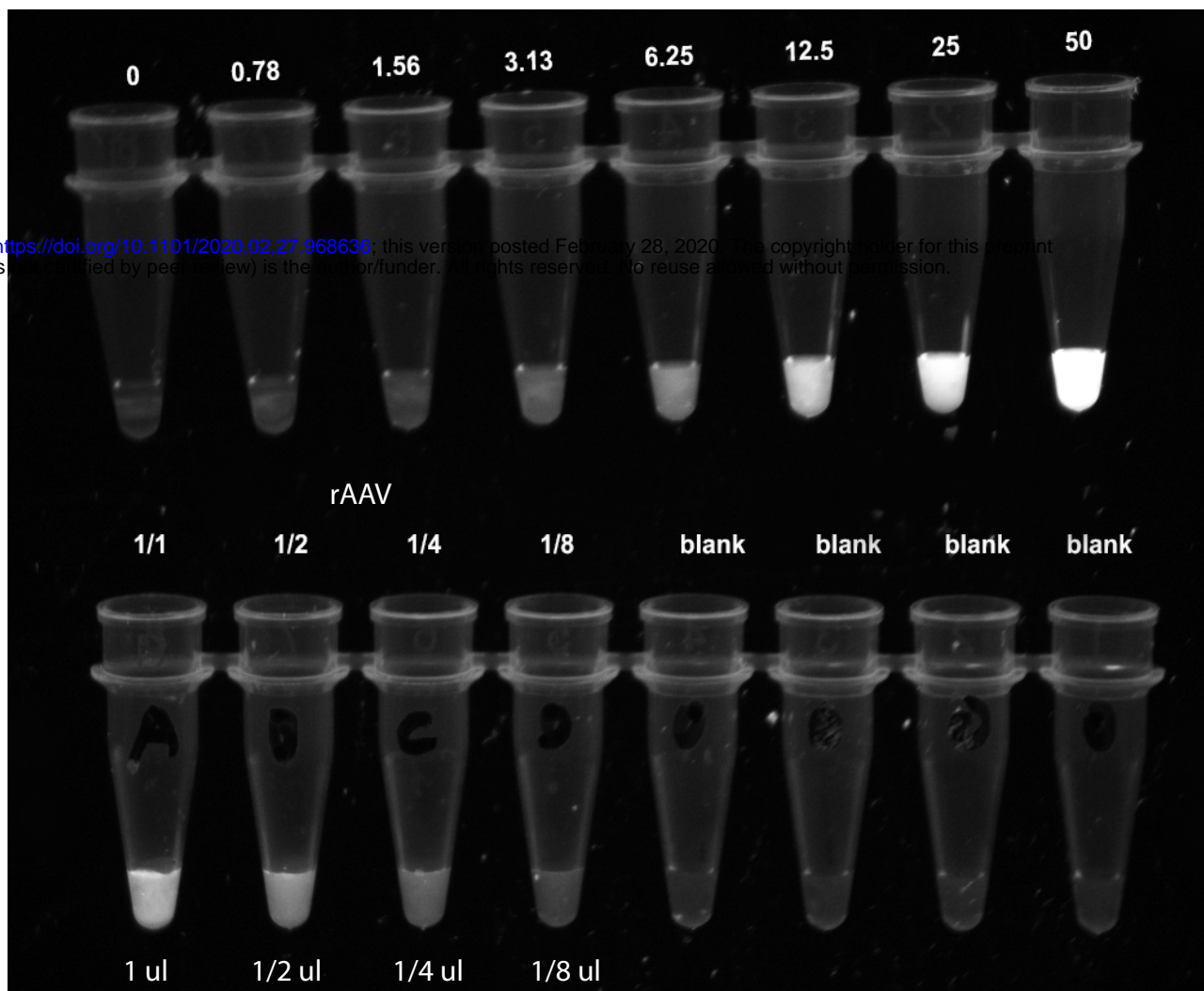


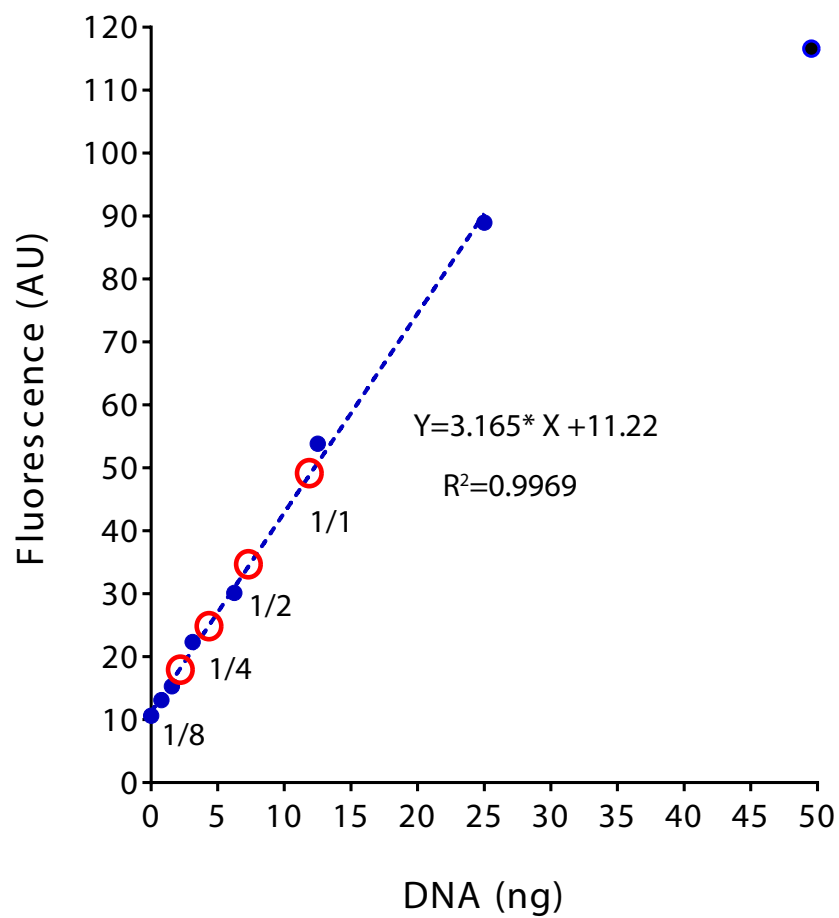
Figure 5

A

DNA standard (ng)



B



C

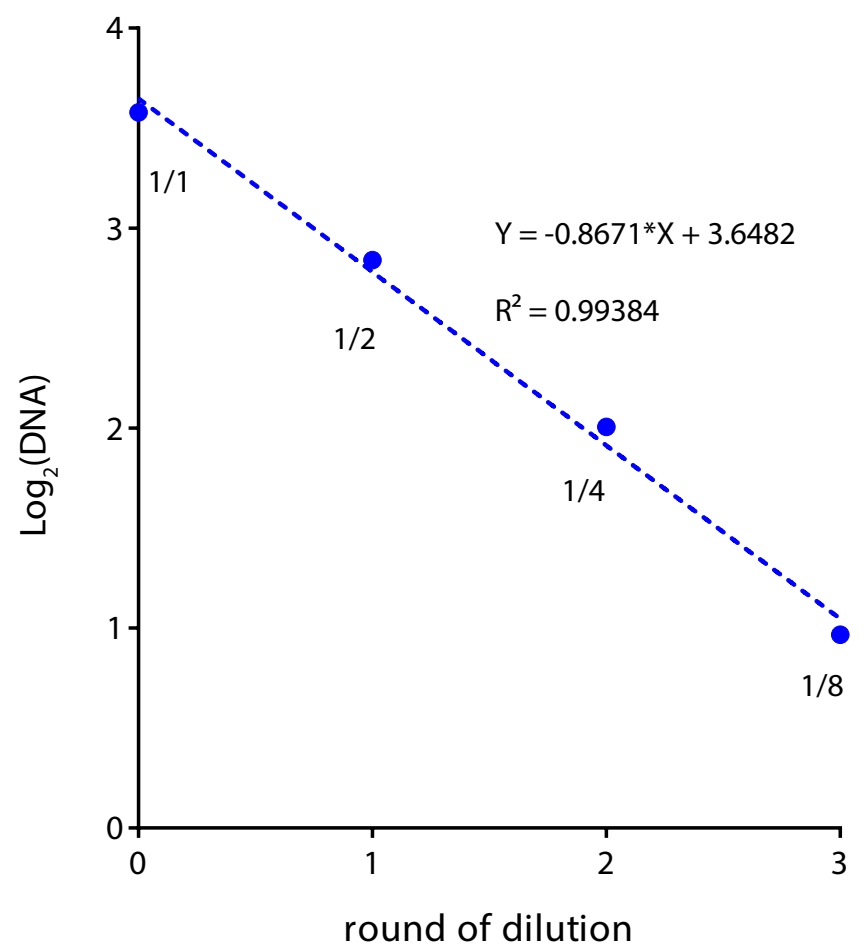


Figure 6



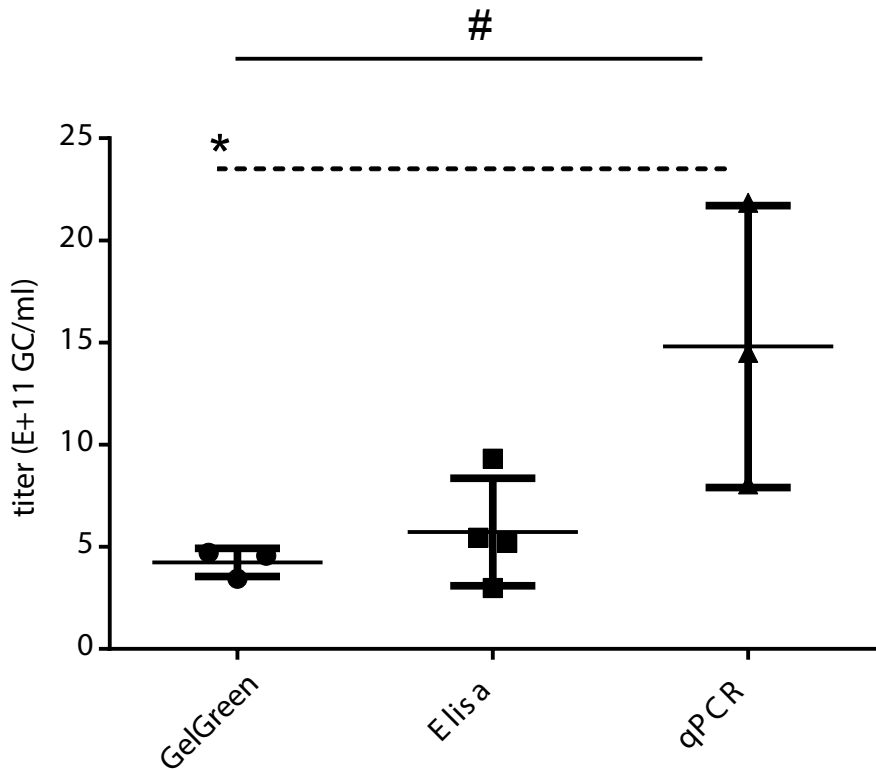


Figure 7

**Table 1. Titration of AAV8RSM (ATCC VR-1816)**

<b>Intra assays</b>								
	<b>Replicate 1</b>	<b>Replicate 2</b>	<b>Replicate 3</b>	<b>Mean</b>	<b>SD</b>	<b>Low 95% CI</b>	<b>High 95% CI</b>	<b>CV%</b>
<b>Assay #1</b>	3.16E+11	3.46E+11	3.69E+11	3.44E+11	2.63E+10	2.78E+11	4.1E+11	7.7
<b>Assay #2</b>	4.71E+11	4.09E+11	4.89E+11	4.56E+11	4.18E+10	3.52E+11	5.6E+11	9.2
<b>Assay #3</b>	4.539E+11	3.41E+11	5.32+011	4.71E+11	1.1E+11	1.92E+11	7.5E+11	16.4
<b>Inter Assays</b>								
	<b>Mean</b>	<b>SD</b>	<b>Low 95%CI</b>	<b>High 95% CI</b>	<b>CV%</b>			
	4.23E+11	6.95E+10	2.51E+11	5.97E+11	16.3			

Titer of the AAV8RSM was determined by GelGreen method. Three independent assays were conducted, with each assay being performed in triplicates. CV, coefficient of variation; CI, confidence interval.